Journal of Biomechanics 44 (2011) 2356–2361

Contents lists available at ScienceDirect

Journal of Biomechanics

journal homepage: www.elsevier.com/locate/jbiomech
www.JBiomech.com

Determination of mechanical properties of soft tissue scaffolds by atomic force microscopy nanoindentation

Yanxia Zhu [a], Zhuxin Dong [b], Uchechukwu C. Wejinya [b], Sha Jin [a], Kaiming Ye [a,*]

[a] Biomedical Engineering Program, College of Engineering, University of Arkansas, 700 Research Center Blvd, 3914 ENRC, Fayetteville, AR 72701, USA
[b] Department of Mechanical Engineering, College of Engineering, University of Arkansas, Fayetteville, AR 72701, USA

ARTICLE INFO

Article history:
Accepted 7 July 2011

Keywords:
AFM
Nanoindentation test
Soft scaffolds
Measurement of mechanical property of scaffolds
3D cultures

ABSTRACT

While the determination of mechanical properties of a hard scaffold is relatively straightforward, the mechanical testing of a soft tissue scaffold poses significant challenges due in part to its fragility. Here, we report a new approach for characterizing the stiffness and elastic modulus of a soft scaffold through atomic force microscopy (AFM) nanoindentation. Using collagen–chitosan hydrogel scaffolds as model soft tissue scaffolds, we demonstrated the feasibility of using AFM nanoindentation to determine a force curve of a soft tissue scaffold. A mathematical model was developed to ascertain the stiffness and elastic modulus of a scaffold from its force curve obtained under different conditions. The elastic modulus of a collagen–chitosan (80%/20%, v/v) scaffold is found to be 3.69 kPa. The scaffold becomes stiffer if it contains more chitosan. The elastic modulus of a scaffold composed of 70% collagen and 30% chitosan is about 11.6 kPa. Furthermore, the stiffness of the scaffold is found to be altered significantly by extracellular matrix deposited from cells that are grown inside the scaffold. The elastic modulus of collagen–chitosan scaffolds increased from 10.5 kPa on day 3 to 63.4 kPa on day 10 when human foreskin fibroblast cells grew inside the scaffolds. Data acquired from these measurements will offer new insights into understanding cell fate regulation induced by physiochemical cues of tissue scaffolds.

1. Introduction

Cells *in vivo* interact with various surrounding cells through cell–cell and cell-extracellular matrix (ECM) interaction in a three dimensional (3D) fashion. It has become clear recently that cell fate is regulated by not only soluble signaling molecules but also by physicochemical cues such as mechanical properties of an ECM. Thus, the determination of mechanical properties of an *in vitro* constructed ECM, i.e., a tissue scaffold, becomes more critical for controlling cell growth and differentiation in 3D environments. A variety of biomaterials have been developed and adopted for fabricating 3D scaffolds. Collagen and chitosan are two widely used natural biomaterials for 3D cultures (Chen et al., 2006; Ma et al., 2003; Yan et al., 2006; Zhang et al., 2006). Both materials can be readily cross-linked to form hydrogels for growing soft tissues (von Heimburg et al., 2001; Wang and Ye, 2009; Zustiak and Leach, 2010). Compared to scaffolds made from hard materials, cells grown inside soft scaffolds respond more significantly to scaffold's mechanical properties (Discher et al., 2009; Engler et al., 2006; Georges and Janmey, 2005; Levental et al., 2007). Besides, the elasticity of the soft scaffolds can be altered by cells through their secreted ECM (Mammoto et al., 2009). Studies suggest that cells can alter substrate's stiffness hundreds of micrometers away from their edges (Winer et al., 2009). The traction forces that cells apply to their matrix can also refashion the matrix stiffness of a hydrogel scaffold that exhibits strain-stiffening behaviors.

Unlike hard scaffolds, the mechanical properties of soft scaffolds are difficult to be characterized due to its fragility. They usually can only tolerate nN stress, making it difficult to measure. One solution is to determine their elastic modulus through indentation. Nanoindentation has been applied for characterizing many soft materials' mechanical properties (Doube et al., 2010; Isaksson et al., 2010). In nanoindentation test, small loads and a small tip can be used with an AFM (Barone et al., 2010). AFM can measure forces at the nN level (Chowdhury and Laugier, 2004; Clifford and Seah, 2006; Darling et al., 2007). For example, AFM nanoindentation has been applied to quantify quasi-static mechanical properties of newly synthesized cell-associated matrices of individual chondrocytes (Lee et al., 2010; Ng et al., 2007). Although AFM nanoindentation shows tremendous potentials for characterizing soft tissues, its application in determining mechanical properties of a hydrogel scaffold in liquid has not yet been explored. Here, we present a new approach of quantifying tensile strength of a soft tissue scaffold using AFM nanoindentation. A mathematical model was developed and used for determining the stiffness and elastic modulus of collagen–chitosan hydrogel scaffolds under various conditions.

* Corresponding author. Tel.: +1 479 575 5315; fax: +1 479 575 2846.
E-mail address: kye@uark.edu (K. Ye).

0021-9290/$ - see front matter © 2011 Elsevier Ltd. All rights reserved.
doi:10.1016/j.jbiomech.2011.07.010

2. Materials and methods

2.1. Scaffold fabrication and cell growth

Collagen–chitosan scaffolds were fabricated, as described previously (Zhu et al., 2009b). In brief, 0.5% (w/v) rat tail type I collagen and 2% chitosan were dissolved in 0.1 M acetic acid, followed by freezing at −80 °C for 2 h and then lyophilized for 24 h. After lyophilization, the scaffolds were cross-linked by cutting them into small sizes (15 mm in diameter and 2 mm in thickness) and immersing into 2 ml 40% (v/v) ethanol containing 50 mM MES (ethanesulfonate) (pH 5.0), 33 mM EDC (carbodiimide) and 8 mM NHS (N-hydroxyl succinimide) for 10 h. After cross-linking, the scaffolds were neutralized with 0.1 M Na_2HPO_4 (pH 9.1) for 1 h, followed by repeatedly washing with 40% ethanol and Milli-Q water to remove excess base until the pH reached 7 to 7.4. The scaffolds were then lyophilized for 24 h and sterilized under UV.

A human foreskin fibroblast cell line, HFF-1 (ATCC SCRC-1041) was routinely maintained in 20% defined fetal bovine serum, 2 mM L-glutamine, 1% nonessential amino acids, 0.1% mM β-mercaptoethanol, and 80% DMEM at 37 °C in a 5% CO_2 incubator. Cells were seeded into collagen–chitosan scaffolds at a density of 1×10^5 cells/scaffold. The scaffolds were pre-washed with PBS buffer and pre-equilibrated with the culture medium.

2.2. SEM

Scaffolds were mounted on stubs with a double-stick carbon tape and sputter coated with gold–palladium, and examined using a Joel Field Emission SEM (JSM-6335F, JOEL) at an accelerating voltage of 5 kV. Distinct sections from each sample were imaged (4 images per sample), and the pore size was determined using the Image-Pro Plus software. At least 90 pores were assessed for each sample. Data are presented as mean pore size ± SD.

2.3. AFM nanoindentation test

The Agilent 5500 ILM AFM was used to perform the AFM nanoindentation test. A rotated monolithic silicon probe with a spring constant of 0.2 N/m was adopted for AFM AC mode imaging and nanoindenting test. The probe employs an "on scan angle" symmetric triangle tip to provide a more symmetric representation of features over 200 nm and its resonance frequency is 13 kHz in air, which could vary accordingly in liquid. The tip radius is about 10 nm and its half cone angle is 25°. The nanoindentation test was done in liquid. For liquid imaging, the laser is aligned in air mode after a tip is assembled. This is critical to the controlling of the distance by which the tip is withdrawn from the sample plate, as the tip and the sample will be invisible after the liquid cell is mounted on the sample plate. After alignment, a liquid cell is mounted on the sample plate to create a liquid-sealed space in which the sample is immersed in a solution. In case the sample floats, a transparent tape can be used to fix the sample to the bottom of the cell to make it stable. The assembled sample plate is then moved to AFM for scanning or indenting. As liquid could cause laser refraction, the position of the detector needs to be carefully adjusted in order to keep receiving signals. The indentation is very much straightforward as the distance between the tip and the sample can be controlled by user. To minimize the chance of producing plastic deformation, a scaffold sample was indented multiple times to obtain the force information, consequently a deformation curve. After locating the sample on the AFM, the sample was indented at several locations within a small neighboring area of the sample surface. Only one indentation was done at each location. The raw data were collected and used for the determination of the tensile strength of the scaffolds.

2.4. Statistical analysis

The mean elastic modulus of a scaffold was determined from its force curve. Data from each group were expressed as the mean ± SD (standard deviation) by frequency analysis. The Levene homogeneity test indicated unequal variances ($p < 0.05$). Therefore, the means were analyzed by one-way analysis of variance with a Brown Forsythe test to account for unequal variances, followed by Bonferroni post-hoc tests using SPSS to evaluate differences between regions. A p-value < 0.05 was considered statistically significant.

3. Results and discussion

Collagen has been widely used in constructing 3D tissue scaffolds (Badylak et al., 2009; Yannas et al., 2010), while chitosan is usually used to endow scaffolds with sufficient mechanical strengths required for cell growth. A number of studies suggest that the mixing of chitosan with collagen can significantly improve cell attachment and proliferation (Gong et al., 2010; Ragetly et al., 2010). Studies further suggest that physicochemical cues of a collagen–chitosan scaffold are significantly different, affected by chitosan content in the scaffolds (Zhu et al., 2009b). We found that a collagen scaffold blended with 20–30% of chitosan provides better cues for cells to grow (Zhu et al., 2009b, 2010). Thus, in this work, the ratios of 8:2 (collagen vs. chitosan) (refer to scaf1) and 7:3 (refer to scaf2) were chosen for fabricating the scaffolds. The SEM images of these two scaffolds are shown in Fig. 1. They both exhibit interconnected network structures with a high porosity. The average pore size is 150 ± 67 μm in scaf1 and 100 ± 48 μm in scaf2. These interconnected porous structures are suitable for cell growth, as reported previously (Lin et al., 2009).

We characterized the mechanical properties of the scaffolds in PBS buffer by the AFM. Fig. 2 illustrates a schematic of the AFM

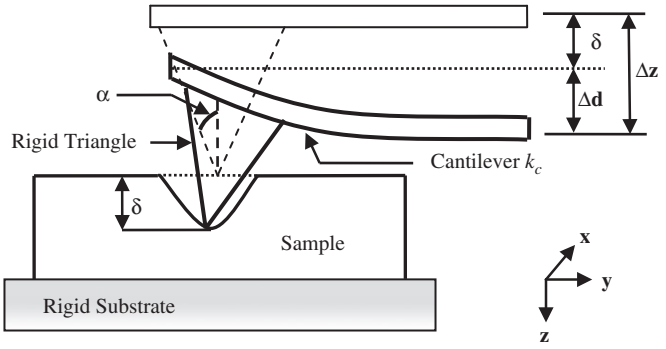

Fig. 2. Schematic of indentation: indentation of a thin biological sample by a triangle probe.

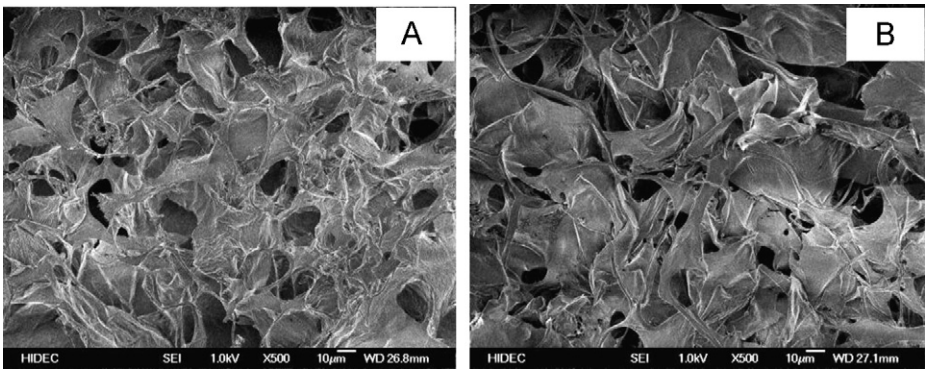

Fig. 1. SEM images of collagen–chitosan scaffolds. Hydrogel scaffolds were prepared by mixing collagen with chitosan in different ratios: (A) 8:2 and (B) 7:3 (collagen–chitosan, v/v). Scale bar: 10 μm.

nanoindentation test. By measuring an indent caused by an AFM tip, a force F (nN) versus the indentation distance (nm) curve can be obtained, from which the Young's or elastic modulus E (Pa) of the scaffold can be determined. Force curves were collected by monitoring the cantilever deflection while ramping the piezo-scanner in z-direction with the xy scanning disabled, resulting in a plot of force versus sample position. As depicted in Fig. 2, Δz is the piezo-actuator translation under user's control, Δd is the deflection of the cantilever, and δ is the indentation distance on the sample. Thus

$$\Delta z = \Delta d + \delta \tag{1}$$

According to the Newton's Third Law, the magnitude of a force acting on the sample is equal to the force exerting on the cantilever; thus

$$F = k_c \Delta d \tag{2}$$

where k_c is the spring constant of an AFM tip cantilever, reflecting the stiffness of the scaffold. On an infinitely stiff sample, the deflection (d) of a cantilever is identical to the movement of the piezo in z-direction, i.e., $d=z$. For a soft sample, a cantilever tip will indent the sample. This indentation (δ) leads to a smaller deflection, i.e., $d=z-\delta$, resulting in a flatter force curve with a smaller slope. d can be determined from the cantilever's contact sensitivity (nm/V) which is determined by indenting mica with the same tip where Δz is equal to Δd (no indentation). The cantilever deflection during indenting a scaffold sample can also be determined from the sensitivity. When indenting the scaffold sample, $\Delta z=\Delta d+\delta$, where Δz is controlled by a user, and Δd is equal to the product of the sensitivity and Amp (V). The Amp can be read from the indentation curve. Assuming $d_0=0$, then $d=\Delta d$.

Because Hooke's Law connects the deflection of a cantilever and its applied loading force *via* the force constant k of the cantilever, the loading force can be given by

$$F = kd = k(z-\delta) \tag{3}$$

While the elastic deformation of two spherical surfaces touching under load can be estimated using a Hertz contact theory and continuum mechanics (Antonyuk et al., 2005), Sneddon mechanical model (Heuberger and Louis, 1996) is more appropriate for a cone pushing onto a flat sample like the one used in this work. Based on this model, the relationship between the indentation δ and the loading force F can be given by

$$F = \left(\frac{2}{\pi}\right)\left[\frac{E}{(1-\nu^2)}\right]\delta^2 \tan(\alpha) \tag{4}$$

where α is the half-opening angle of an AFM tip, and ν is the Poisson's ratio. As

$$\Delta z = z - z_0 \tag{5}$$

$$\Delta d = d - d_0 \tag{6}$$

$$\delta = \sqrt{\frac{F}{[(2/\pi)(E/(1-\nu^2))\tan(\alpha)]}} \tag{7}$$

and

$$F = k(d-d_0) \tag{8}$$

By combining these equations yields

$$z - z_0 = d - d_0 + \sqrt{k(d-d_0)/\{2E\tan(\alpha)/[\pi(1-\nu^2)]\}} \tag{9}$$

To determine an elastic modulus from this equation, the zero deflection (d_0) has to be determined in the noncontact part of a force curve. Because the scaffold obeys rubber elasticity, we assumed a Poisson ratio of 0.5 (Baldwin et al., 1955). We used 0.2 N/m as a determined force constant and 25° as the half-opening angle of the cone, based on specifications of the AFM provided by the manufacturer. Now only two variables, i.e., the contact point z_0 and the elastic modulus E are unknown in Eq. (9). These two variables can be determined independently by taking two different deflection values and their corresponding z values from a force curve. These two data points define the range of deflection values, corresponding to a range of loading force.

Because the AFM tips used are rather sharp cones, the induced shear stress is on the order of the sample's elastic modulus with the danger of producing plastic deformation. Although the cone could penetrate the surface of a scaffold, resulting in plastic and/or irreproducible deformations, such effect can be minimized by taking a reading on one spot a time. We believe that as long as the indentation approach and retrace plots are the same for one and the other, and the force curves obtained are linear, the elastic state would be guaranteed. Fig. 3 presents the force curves from 4 indentations on scaf1. The slopes (nN/nm) are 0.01058 (indentation 1), 0.008055 (indentation 2), 0.02341 (indentation 3), and 0.01845 (indentation 4). They seem to be within a reasonable range. Next, we investigated whether an indenting approach is identical to a retraction curve. Fig. 4 shows a typical set of raw data of one of the indentation experiments performed using scaf2. It appears that the approach and the retrace curves are not completely overlapped. There is a 0.4 μm offset between the start and end height. The effect of this offset, however, is minor, as the indenting curves are linear. This offset could be due to some deficiencies, such as elastic hysteresis or water attraction force. As the measurements were performed in PBS buffer, water can hold the tip when the scanner is pulled away from the surface, leading to the offset shown in Fig. 4. A similar phenomenon has been described in the literatures (Howland and Benatar, 2000). Based on these measurements, we assumed that the deformation during indentation is elastic and the indenter is a rigid body. Only the approach data are used for obtaining force curves of a sample.

On the other hand, the radius of a tip used in AFM indentation is less than 10 nm, while the features on the scaffolds tested are in dimensions of 10 μm scale (Fig. 1). Thus, we assumed that the tip is indenting a flat surface, which satisfies the schematic in Fig. 2

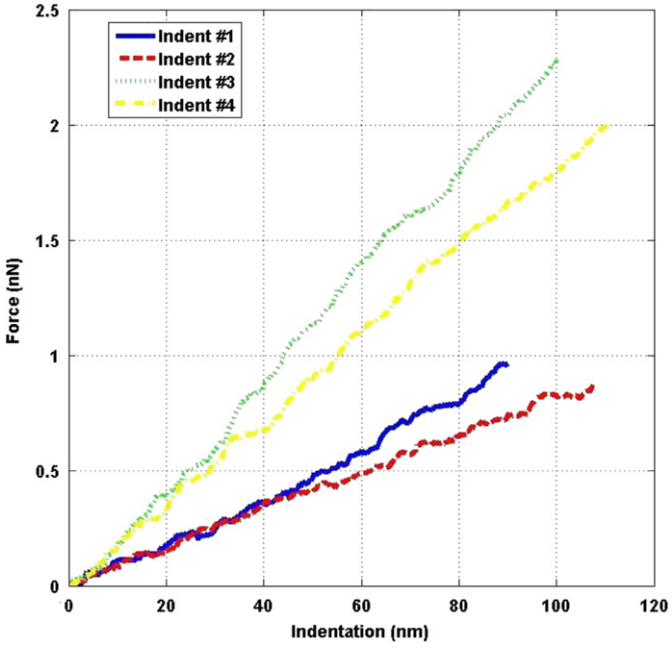

Fig. 3. Force curves obtained from indenting collagen–chitosan (at a ratio of 8:2) scaffolds at multiple locations within a small neighboring area of the sample surface. Only one indentation was performed at each location.

as well as Eq. (4). It is noteworthy to point out that Fig. 4 presents a load–displacement curve of a cantilever used for indenting a scaffold. It was plotted by the load on the cantilever versus the piezo-actuator translation in the *z*-direction but not the load on the cantilever versus the cantilever deflection.

Before plotting a force curve, the sensitivity (nm/V) of the AFM needs to be determined; thus, we indented a mica surface using the same tip. The mica surface is hard enough to be considered as a rigid substrate; thus, the translation distance is equal to the deflection of the cantilever. From these tests, we resolved the sensitivity of the AFM. It is approximately 89 nm/V.

Due to the viscosity of hydrogel scaffolds in PBS buffer, hydrodynamic drag force could add a constant external force to the loading force of a cantilever. This force can, however, be separated by reducing the scanning speed of the tip. By indenting slowly enough, the viscous contributions will be very small. Then, the force measurements will only be dominated by elastic behaviors of the materials. The force curves were obtained in the contact mode at a lateral scanning speed of 0.5 line/s. While indenting, there is no speed control, but the indentation distance and the total number of data points along that distance are controlled. For example, the indentation distance is 5 μm and the number of data points, which possess the indenting information, is 10,000. The scanning speed was determined empirically and considered to be slow enough to minimize the amount of hysteresis, yet fast enough to maximize the number of force curves that can be captured in a given measurement. We used 50–75% of the approaching curve to calculate the indentation, as the use of the retracting curve leads to an incorrect measurement of indentation.

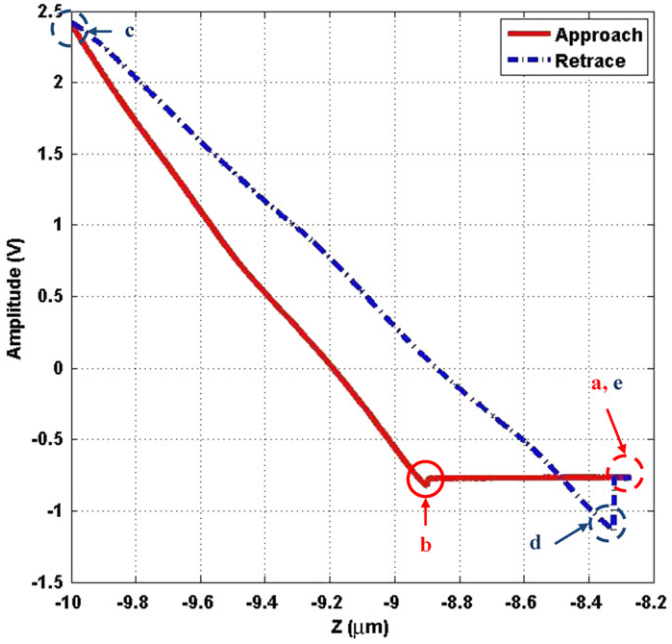

Fig. 4. AFM raw data of indenting a collagen–chitosan (at a ratio of 7:3) scaffold. (a) Piezo-movement starts in the *z*-axis; (b) cantilever begins to contact the sample; (c) *z*-axis movement stops; (d) cantilever departs from the sample during unloading; and (e) piezo-movement stops.

With these settings, we determined the force curves of both scaf1 and scaf2 scaffolds (Fig. 5). To validate these tests, we ascertained the mechanical properties of mouse pancreas and heart tissues prepared from 3 mice. The measurement showed that the average elastic modulus of mouse heart and pancreas tissues is about 47.4 and 8.25 kPa, respectively (Fig. 6b). These measurements are in agreement with others work. For example, one study shows that the average stiffness of a mouse heart sample is about 49.6 kPa (http:www.mate.tue.nl/mate/pefs/9706.pdf). Thus, we believe that the test developed in this work is reliable for characterizing scaffolds' mechanical properties. After these validations, we determined the mechanical properties of both scaf1 and scaf2 (Fig. 6a). The elastic modulus of scaf2 is 11.6 kPa, whereas it is 3.96 kPa for scaf1 (Fig. 6), suggesting that the addition of chitosan to a collagen scaffold helps enhance its stiffness. These elastic moduli were determined from six force curves for each sample.

Next, we investigated whether the tensile strength of a collagen–chitosan scaffold is altered by ECM deposited from cells grown inside a scaffold. We seeded the human foreskin fibroblasts into both scaf1 and scaf2, as reported previously (Zhu et al., 2009b, 2010). The elastic moduli of the two scaffolds were determined at different time points within 10 days of cultures. As shown in Fig. 7a and b, their elastic moduli decreased gradually when they were immersed in a cell culture medium for 10 days. The scaf1's elastic modulus dropped from 3.69 to 2.63 kPa, while scaf2's elastic modulus declined from 11.6 to 5.19 kPa after 10 days incubation. It appears that a high content collagen in the scaffolds helps delay their deterioration. As documented in literatures, collagen tends to degrade in culture medium (Serpooshan et al., 2010; Yannas et al., 2010). In contrast, the tensile strength of collagen–chitosan scaffolds increased when

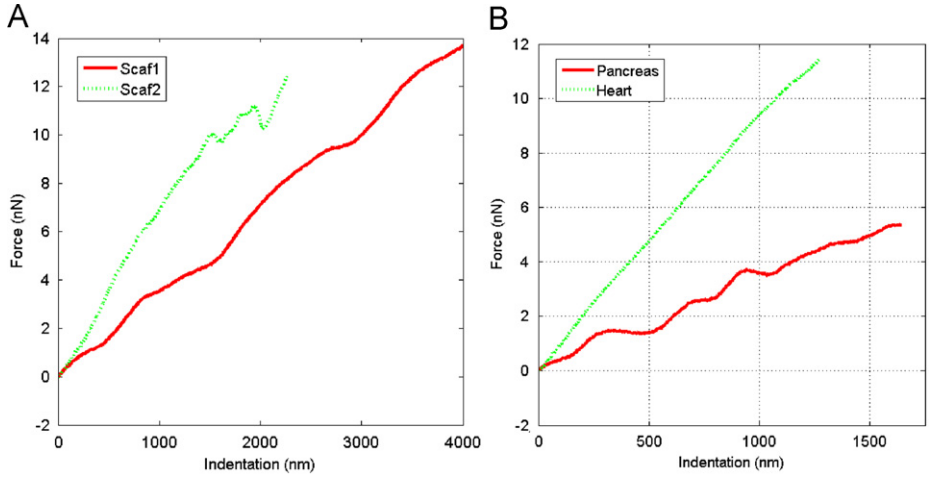

Fig. 5. Force curves of scaffolds determined through AFM nanoindentation test. (A) Force curves of two scaffolds prepared using different ratios: scaf1, 8:2 and scaf2, 7:3 (collagen–chitosan, v/v). (B) Force curves of mouse pancreas and heart tissues used as controls for AFM nanoindentation.

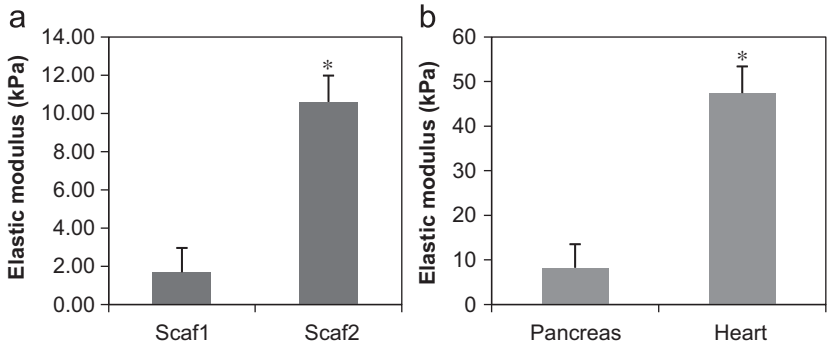

Fig. 6. Elastic moduli of scaffolds and mouse tissue samples determined through AFM nanoindentation test. (a) Collagen–chitosan scaffolds. (b) Mouse pancreas and heart tissue samples. Data are presented as mean ± SD of 6 measurements for each scaffold or tissue sample. $^{*}p < 0.05$.

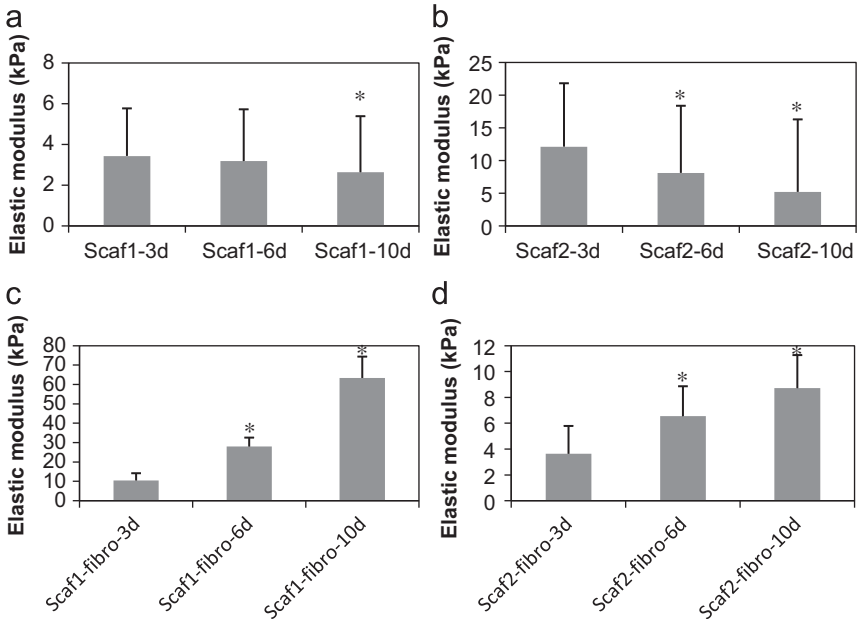

Fig. 7. Changes in elastic moduli of scaffolds during 3D cell cultures. Elastic moduli of Scaf1 (collagen–chitosan ratio is 8:2 (v/v)) (a) and Scaf2 (collagen–chitosan ratio is 7:3 (v/v)) (b) were determined through AFM nanoindentation test at day 3, day 6, and day 10 when they are incubated in cell culture medium. The elastic moduli of scaf1 (c) and scaf2 (d) in which human embryonic fibroblast cells were cultured were also determined at day 3, day 6, and day 10. Data presented are mean ± SD of 6 measurements for each scaffold. $^{*}p < 0.05$.

cells were grown inside them. The elastic modulus of scaf1 was elevated from 10.5 kPa on day 3 to 63.4 kPa on day 10 when the human foreskin fibroblasts were cultured inside the scaffolds (Fig. 7c). The deposition of ECM from cells might contribute to this increase. Although we did not directly observe the cellular deposition of ECM in this work, our early work using similar scaffolds demonstrated the ECM deposition from cells grown inside the scaffolds (Zhu et al., 2009a, 2009b, 2010). Moreover, we found that the tensile strength of a collagen–chitosan scaffold is less affected by the cellular deposition of ECM if a high content chitosan is used for fabricating scaffolds (Fig. 7d). The elastic modulus of scaf2 was increased only slightly from 3.64 kPa on day 3 to 8.72 kPa on day 10 with cells grown inside the scaffolds.

The cellular enhancement of mechanical properties of a collagen scaffold has been observed by other groups as well. For example, the deposition of ECM from cells was found to enhance the tensile strength of a collagen sponge scaffold (Orwin et al., 2003). The transition of mechanical property has been found in other scaffolds as well. For example, the protein adsorption to the alginate during cell culture led to an increase in mechanical properties of a porous alginate scaffold seeded with hepatocytes or fibroblast-like cells (Sakai et al., 2005). The effect of scaffold stiffness on cells has also been characterized extensively. For example, cell organization, myotube formation, and cell viability have been found to be affected significantly by scaffold stiffness for myoblasts grown and differentiated in 3D ploy-lactic acid (PLLA)/poly(lactic-co-glycolic acid) (PLGA) porous scaffolds (Levy-Mishali et al., 2009). The elasticity of these scaffolds was controlled by adjusting the ratio of PLLA vs. PLGA in the scaffolds. They found that PLLA-containing scaffolds (100–25% PLLA) provide stiffness that supports myotube formation. It is also noteworthy to point out that large variation in elastic modulus measurements was observed in our experiment. We reasoned that these variations might be due to the nature of porous scaffolds or due to the different positions where a tip touched the scaffolds during the measurements. Thus, the procedure needs to be further optimized in order to generate more consistent measurements. In summary, we here demonstrated that an AFM tation test can be conducted in a liquid fashion for characterizing mechanical properties of a soft tissue scaffold. These data would offer new insights into tailoring physicochemical cues for enhancing cell growth and differentiation in 3D environments.

Conflict of interest statement

We herein declare that none of authors involved in this work have conflict of interest.

Acknowledgments

This work is partially supported by the National Science Foundation Grant NSF CBET 0756455, Juvenile Diabetes Research Foundation Grant 5-2009-381, and ABI Grant 0152-27504-231108.

References

Antonyuk, S., Tomas, J., Heinrich, S., Morl, L., 2005. Breakage behavior of spherical granulates by compression. Chem. Eng. Sci. 60, 4031–4044.
Badylak, S.F., Freytes, D.O., Gilbert, T.W., 2009. Extracellular matrix as a biological scaffold material: structure and function. Acta Biomater. 5, 1–13.
Baldwin, F.P., Ivory, J.E., Anthony, R.L., 1955. Experimental examination of the statistical theory of rubber elasticity: low extension studies. J. Appl. Phys. 26, 750–756.
Barone, A.C., Salerno, M., Patra, N., Gastaldi, D., Bertarelli, E., Carnelli, D., Vena, P., 2010. Calibration issues for nanoindentation experiments: direct atomic force microscopy measurements and indirect methods. Microsc. Res. Technol. 73, 996–1004.
Chen, R.N., Wang, G.M., Chen, C.H., Ho, H.O., Sheu, M.T., 2006. Development of N,O-(carboxymethyl)chitosan/collagen matrixes as a wound dressing. Biomacromolecules 7, 1058–1064.
Chowdhury, S., Laugier, M.T., 2004. The use of non-contact AFM with nanoindentation techniques for measuring mechanical properties of carbon nitride thin films. Appl. Surf. Sci. 233, 219–226.
Clifford, C.A., Seah, M.P., 2006. Modeling of nanomechanical nanoindentation measurements using an AFM or nanoindenter for compliant layers on stiffer substrates. Nanotechnology 17, 5283–5292.
Darling, E.M., Zauscher, S., Block, J.A., Guilak, F., 2007. A thin-layer model for viscoelastic, stress-relaxation testing of cells using atomic force microscopy: do cell properties reflect metastatic potential? Biophys. J. 92, 1784–1791.
Discher, D., Dong, C., Fredberg, J.J., Guilak, F., Ingber, D., Janmey, P., Kamm, R.D., Schmid-Schonbein, G.W., Weinbaum, S., 2009. Biomechanics: cell research and applications for the next decade. Ann. Biomed. Eng. 37, 847–859.
Doube, M., Firth, E.C., Boyde, A., Bushby, A.J., 2010. Combined nanoindentation testing and scanning electron microscopy of bone and articular calcified cartilage in an equine fracture predilection site. Eur. Cell Mater. 19, 242–251.
Engler, A.J., Sen, S., Sweeney, H.L., Discher, D.E., 2006. Matrix elasticity directs stem cell lineage specification. Cell 126, 677–689.
Georges, P.C., Janmey, P.A., 2005. Cell type-specific response to growth on soft materials. J. Appl. Physiol. 98, 1547–1553.
Gong, Z., Xiong, H., Long, X., Wei, L., Li, J., Wu, Y., Lin, Z., 2010. Use of synovium-derived stromal cells and chitosan/collagen type I scaffolds for cartilage tissue engineering. Biomed. Mater. 5, 055005.
Heuberger, M.D., Louis, G.S., 1996. Elastic deformations of tip and sample during atomic force microscope measurements. J. Vac. Sci. Technol. B: Microelectron. Nanometer Struct. 14, 1250–1254.
Howland, R., Benatar, L., 2000. A practical guide to scanning probe microscopy. In: Symanski, C. (Ed.), Thermo Microscopes. Sunnyvale, CA.
Isaksson, H., Nagao, S., Malkiewicz, M., Julkunen, P., Nowak, R., Jurvelin, J.S., 2010. Precision of nanoindentation protocols for measurement of viscoelasticity in cortical and trabecular bone. J. Biomech. 43, 2410–2417.
Lee, B., Han, L., Frank, E.H., Chubinskaya, S., Ortiz, C., Grodzinsky, A.J., 2010. Dynamic mechanical properties of the tissue-engineered matrix associated with individual chondrocytes. J. Biomech. 43, 469–476.
Levental, I., Georges, P.C., Janmey, P., 2007. Soft biological materials and their impact on cell function. Soft Matter 3, 299–306.
Levy-Mishali, M., Zoldan, J., Levenberg, S., 2009. Effect of scaffold stiffness on myoblast differentiation. Tissue Eng. Part A 15, 935–944.
Lin, Y.C., Tan, F.J., Marra, K.G., Jan, S.S., Liu, D.C., 2009. Synthesis and characterization of collagen/hyaluronan/chitosan composite sponges for potential biomedical applications. Acta Biomater. 5, 2591–2600.
Ma, L., Gao, C., Mao, Z., Zhou, J., Shen, J., Hu, X., Han, C., 2003. Collagen/chitosan porous scaffolds with improved biostability for skin tissue engineering. Biomaterials 24, 4833–4841.
Mammoto, A., Connor, K.M., Mammoto, T., Yung, C.W., Huh, D., Aderman, C.M., Mostoslavsky, G., Smith, L.E., Ingber, D.E., 2009. A mechanosensitive transcriptional mechanism that controls angiogenesis. Nature 457, 1103–1108.
Ng, L., Hung, H.H., Sprunt, A., Chubinskaya, S., Ortiz, C., Grodzinsky, A., 2007. Nanomechanical properties of individual chondrocytes and their developing growth factor-stimulated pericellular matrix. J. Biomech. 40, 1011–1023.
Orwin, E.J., Borene, M.L., Hubel, A., 2003. Biomechanical and optical characteristics of a corneal stromal equivalent. J. Biomech. Eng. 125, 439–444.
Ragetly, G.R., Griffon, D.J., Lee, H.B., Fredericks, L.P., Gordon-Evans, W., Chung, Y.S., 2010. Effect of chitosan scaffold microstructure on mesenchymal stem cell chondrogenesis. Acta Biomater. 6, 1430–1436.
Sakai, S., Masuhara, H., Yamada, Y., Ono, T., Ijima, H., Kawakami, K., 2005. Transition of mechanical property of porous alginate scaffold with cells during culture period. J. Biosci. Bioeng. 100, 127–129.
Serpooshan, V., Julien, M., Nguyen, O., Wang, H., Li, A., Muja, N., Henderson, J.E., Nazhat, S.N., 2010. Reduced hydraulic permeability of three-dimensional collagen scaffolds attenuates gel contraction and promotes the growth and differentiation of mesenchymal stem cells. Acta Biomater. 6, 3978–3987.
von Heimburg, D., Zachariah, S., Heschel, I., Kuhling, H., Schoof, H., Hafemann, B., Pallua, N., 2001. Human preadipocytes seeded on freeze-dried collagen scaffolds investigated in vitro and in vivo. Biomaterials 22, 429–438.
Wang, X., Ye, K., 2009. Three-dimensional differentiation of embryonic stem cells into islet-like insulin-producing clusters. Tissue Eng. Part A 15, 1941–1952.
Winer, J.P., Oake, S., Janmey, P.A., 2009. Non-linear elasticity of extracellular matrices enables contractile cells to communicate local position and orientation. PLoS One 4, e6382.
Yan, J., Li, X., Liu, L., Wang, F., Zhu, T.W., Zhang, Q., 2006. Potential use of collagen–chitosan–hyaluronan tri-copolymer scaffold for cartilage tissue engineering. Artif. Cells Blood Substit. Immobil. Biotechnol. 34, 27–39.
Yannas, I.V., Tzeranis, D.S., Harley, B.A., So, P.T., 2010. Biologically active collagen-based scaffolds: advances in processing and characterization. Philos. Trans. A Math. Phys. Eng. Sci. 368, 2123–2139.
Zhang, Y., Cheng, X., Wang, J., Wang, Y., Shi, B., Huang, C., Yang, X., Liu, T., 2006. Novel chitosan/collagen scaffold containing transforming growth factor-beta1 DNA for periodontal tissue engineering. Biochem. Biophys. Res. Commun. 344, 362–369.
Zhu, J., Sabharwal, T., Kalyanasundaram, A., Guo, L., Wang, G., 2009a. Topographic mapping and compression elasticity analysis of skinned cardiac muscle fibers in vitro with atomic force microscopy and nanoindentation. J. Biomech. 42, 2143–2150.
Zhu, Y., Liu, T., Song, K., Jiang, B., Ma, X., Cui, Z., 2009b. Collagen–chitosan polymer as a scaffold for the proliferation of human adipose tissue-derived stem cells. J. Mater. Sci.: Mater. Med. 20, 799–808.
Zhu, Y., Liu, T., Ye, H., Song, K., Ma, X., Cui, Z., 2010. Enhancement of adipose-derived stem cell differentiation in scaffolds with IGF-I gene impregnation under dynamic microenvironment. Stem Cells Dev. 19, 1547–1556.
Zustiak, S.P., Leach, J.B., 2010. Hydrolytically degradable poly(ethylene glycol) hydrogel scaffolds with tunable degradation and mechanical properties. Biomacromolecules 11, 1348–1357.